





Enhancing Geographic Greedy Routing in Sparse LDACS Air-to-Air Networks through k -Hop Neighborhood Exploitation

Musab Ahmed , Konrad Fuger , Koojana Kuladinithi , Andreas Timm-Giel 
Hamburg University of Technology, Institute of Communication Networks, Hamburg, Germany

Abstract—The emergence of the L -band Digital Aeronautical Communications System (LDACS) presents a significant opportunity for enabling Air-to-Air (A2A) communication to accommodate the growing number of aircraft. However, it requires overcoming significant Medium Access Control (MAC) delays and enhancing connectivity in sparse networks. Geographic greedy routing, commonly used in Aeronautical Ad-hoc networks, utilizes position information to eliminate the need for topology discovery. Yet, its efficacy declines as network density decreases. With the gradual introduction of aircraft equipped with LDACS, it becomes crucial to improve greedy forwarding performance. This research investigates Greedy- k , a greedy forwarding variant using k -hop neighborhood information, to boost sparse network performance. We introduce a method to minimize beacon size by transmitting a subset of k -hop neighborhood data that fits within an LDACS time slot. We derived the subset size analytically and evaluated the performance through simulations benchmarked against the conventional Greedy-1. Our results indicate that the proposed approach achieves up to 13% higher Packet Delivery Ratio (PDR) than Greedy-1, while capturing additionally 70.1% and 34.6% of 2nd and 3rd order neighbors, respectively.

Index Terms—geographic routing, greedy forwarding, A2A, LDACS

I. INTRODUCTION

By the year 2050, the European Organisation for the Safety of Air Navigation (EUROCONTROL) forecasts a 44% increase in flight numbers compared to 2019, necessitating advanced communication technologies for safety, data rate, and reliability [1]. The L -band Digital Aeronautical Communications System (LDACS), currently under standardization, is proposed as a solution for Air-to-Ground (A2G) communication within the Future Communications Infrastructure (FCI), potentially enhancing data rates by up to 200% [2]. It is also proposed to be extended for Air-to-Air (A2A) communication [3].

Recently, the Multi-Channel Self-Organized Time-Division Multiple Access (MCSOTDMA) protocol has been proposed as a viable Medium Access Control (MAC) layer for LDACS A2A communications [4]. This protocol utilizes a Shared (SH) channel for broadcasting beacons and multiple Point-to-Point (PP) channels for unicast packets, ensuring deterministic delays. Geographic routing, the state-of-the-art routing protocol for A2A communication [5], uses beacons to transmit positional information and routes packets greedily towards their destination. If a packet reaches a dead-end, it is dropped or requires a backup

mechanism to continue. In deploying LDACS for A2A communications, we identify two key challenges.

Challenge I: The practical implementation of LDACS for A2A links is expected to be a long process, starting by integrating the technology into newly built aircraft. The airspace will include both legacy and LDACS-equipped aircraft until full LDACS deployment is achieved. This situation raises concerns about LDACS A2A performance in sparse networks, particularly regarding the coexistence with legacy aircraft over the coming decades.

Challenge II: In the SH channel, a Randomized Slotted ALOHA (RS-ALOHA) is used [6]. This results in a MAC delay that increases linearly with the number of neighboring aircraft. Using a high communication range increases the number of direct neighbors, resulting in significant MAC delays affecting both SH and PP links. To accommodate future growth in airspace, reducing the communication range while ensuring high connectivity with ground stations can mitigate these delays. However, this reduction requires improvements in greedy routing to ensure routes are found when they exist topologically.

This paper proposes a solution that can cope with both difficulties. Greedy forwarding, a main component of geographic routing, while effective in dense airspace [7], struggles with frequent dead-ends in sparse networks as shown in Figure 5. Greedy- k , is proposed as an enhancement in such environments by using extended k -hop neighborhood information [8], [9]. However, this approach results in beacons that exceed the capacity of an LDACS A2A slot in the SH channel. Therefore, we introduce a method that optimizes the beacon size by including only a subset of the neighborhood, facilitating more efficient and scalable Greedy- k implementation in sparse network scenarios.

Our main contributions are:

- We analytically derive an optimal fixed subset size to improve Greedy-1 forwarding performance.
- We propose three subset selection methods (*Random*, *Farthest First (FF)* traversal, and *Extended Farthest First (EFF)* traversal) and introduce a geographic greedy routing protocol that uses this information.
- We evaluate our proposed routing protocol and selection methods over the French airspace with varying equipage fractions, reflecting initial and extended use of LDACS-equipped aircraft in the future.

The organization of the paper is as follows: The required subset size is discussed in Section II. The proposed geographic routing protocol is introduced in Section III. The simulation setup is outlined in Section IV. Our results and discussions are detailed in Section V. Related work is discussed in Section VI. The conclusion and further insights on future directions are given in Section VII.

II. THE SUBSET SIZE OF THE K-HOP NEIGHBORHOOD

To optimize Greedy-2 routing performance, a node requires a subset of its 1-hop neighborhood, denoted as $\mathcal{S}_{a_i}^1$, from the full set $\mathcal{N}_{a_i}^1$ where $\mathcal{N}_{a_i}^1$ are 1st order neighbors of a_i in network \mathcal{A} . The challenge lies in determining the optimal subset size $m = |\mathcal{S}_{a_i}^1|$ that maximizes coverage while minimizing redundancy.

Coverage is modeled in Two-dimensional (2D) space using a Unit Disc Graph (UDG). Although aircraft operate in Three-dimensional (3D) space, the altitude variation is minor compared to their communication range r . We consider an infinite set $\mathcal{N}_{a_i}^1$, uniformly distributed within the communication range. To maximize diversity, we ensure that m selected nodes are maximally distant from each other and from node a_i . We analyze various m values, assessing their impact on coverage and overlap, where coverage is the area beyond a_i 's range relative to the 2nd order neighbor area ($3\pi r^2$), and overlap is the area shared between the nodes' coverage. The case for $m = 4, 6$ is demonstrated in Figure 1, where the Coverage is depicted by the grey hashed area (75.72%, 88.41%) and Overlap by the dark grey hashed area (5.41%, 33.28%) respectively.

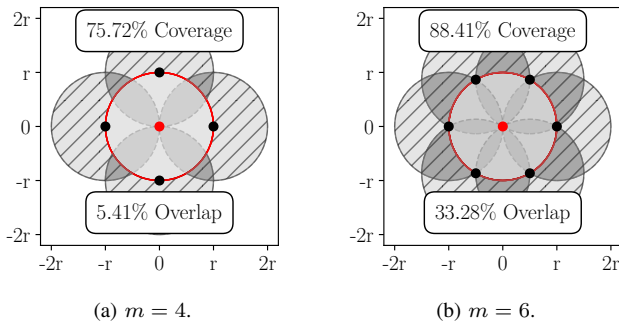


Fig. 1: Coverage and overlap for subset sizes $m = 4$ and $m = 6$, where the node a_i is depicted in red.

Furthermore, we analyzed various m values to assess their effects on coverage, overlap, the rate of change of coverage ($\Delta\text{Coverage}$) and the rate of change of overlap ($\Delta\text{Overlap}$), as depicted in Figure 2. Here, increasing m enhances coverage, yet $\Delta\text{Coverage}$ decreases after $m = 3$ as overlap among nodes starts. When $m > 4$, we see that $\Delta\text{Coverage} < \Delta\text{Overlap}$, which means the redundancy among selected nodes increases faster than the increase in coverage. In this study, we establish $m = |\mathcal{S}_{a_i}^1| = 4$ to optimally distribute coverage around a_i , maintaining $\Delta\text{Coverage} > \Delta\text{Overlap}$.

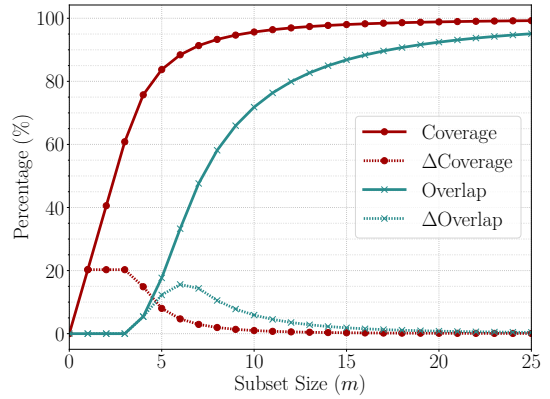


Fig. 2: Illustration of coverage (Coverage) and overlap (Overlap) areas, along with their rates of change ($\Delta\text{Coverage}$ and $\Delta\text{Overlap}$), for different subset sizes m .

III. GEOGRAPHIC GREEDY ROUTING WITH A SUBSET OF K-HOP NEIGHBORHOOD

A. System Model

Within the routing algorithm, a_c denotes the current node. Each node $a_c \in \mathcal{A}$ receives beacons B_{a_s} from beacon senders $a_s \in \mathcal{N}_{a_c}^1$. Beacons include the sender's address a_s , position p_{a_s} , sequence number seq_{a_s} , and neighbor subset information. For each neighbor a_i in this subset, its address, position p_{a_i} , hop count h_{a_i} , and sequence number seq_{a_i} are in B_{a_s} . A beacon entry occupies 12 B, 4 B for the node address (1 B prefix plus 24 bit International Civil Aviation Organization (ICAO) ID), 6 B for the position in Compact Position Reporting (CPR) format, 1 B for hop count, and 1 B for the sequence number. Sequence numbers, incremented by each node $a_c \in \mathcal{A}$ upon $\mathcal{N}_{a_c}^1$ changes, track direct neighbor additions or removals.

Nodes maintain a position table \mathcal{T}_{a_c} , contains all neighbors \mathcal{N}_{a_c} known through received beacons. Each entry $a_i \in \mathcal{T}_{a_c}$ includes a_i 's address, position p_{a_i} , hops to a_i h_{a_i} , sequence number seq_{a_i} , via address via_{a_i} (indicating the beacon's sender) and validity time t_{a_i} , calculated as:

$$t_{a_i} = t_{B_{a_s}} + t_{\text{validity}}, \quad (1)$$

where $t_{B_{a_s}}$ is the beacon reception time and t_{validity} is a pre-defined beacon interval. An example of a node's position table is shown in Table I.

TABLE I: Position Table of a_c (\mathcal{T}_{a_c})

\mathbf{a}_i	$\mathbf{p}_{\mathbf{a}_i}$	$\mathbf{h}_{\mathbf{a}_i}$	$\text{seq}_{\mathbf{a}_i}$	$\text{via}_{\mathbf{a}_i}$	$\mathbf{t}_{\mathbf{a}_i}$
a_1	(x_1, y_1, z_1)	2	22	a_2	20.5 s
a_2	(x_2, y_2, z_2)	1	34	a_2	24 s
...

B. Neighbor Selection Mechanism

In this section, we describe three methods for selecting a subset $\mathcal{S}_{a_c}^k \subseteq \mathcal{N}_{a_c}^k$, where each neighbor is exactly k -hop away from node a_c . The first method, *Random*, randomly

selects neighbors to form a subset of size m . This serves as a baseline strategy.

The second method, the *FF* algorithm, starts by randomly picking an initial node and then iteratively adds the node farthest from those already selected, until m nodes are chosen or all potential nodes are exhausted. This strategy optimizes spatial diversity among the selected nodes and functions as a standard farthest-first selection. The *FF* algorithm can also incorporate a set of preselected elements $\mathcal{S}_{a_c}^{\text{pre}}$, where it starts from this set instead of from a random element. Then the preselected nodes are removed in later steps. The notation $\text{FF}(\mathcal{N}_{a_c}^k, m, \mathcal{S}_{a_c}^{\text{pre}} = \emptyset)$ represents the *FF* algorithm when used without $\mathcal{S}_{a_c}^{\text{pre}}$.

The *EFF* method, denoted by $\text{EFF}(\mathcal{N}_{a_c}^k, m, d_{\text{thr}}, d_{\text{thr},c})$, enhances the *FF* strategy by integrating a distance threshold, d_{thr} , and a distance to current node, $d_{\text{thr},c}$. The threshold ensures that no two nodes within the subset are closer than the specified distance, reducing redundancy. For a subset size of $m = 4$, optimal for 1st order neighbors, d_{thr} is set to $\frac{1}{\sqrt{2}} \cdot r$. This value ensures that nodes diagonally positioned within a square remain outside each other's communication range, effectively minimizing overlap. Similarly, $d_{\text{thr},c}$ is established at $\frac{1}{2} \cdot r$, corresponding to the radius of the circle in which the square, centered at a_c with its diagonal nodes at the edge of each other's communication range, is inscribed. Applying the thresholds d_{thr} and $d_{\text{thr},c}$ might result in selecting fewer than m nodes due to the spatial arrangement of neighbors. This approach allows us to extend our selection to $k + 1$ th order neighbors $\mathcal{N}_{a_c}^{k+1}$, as will be discussed in Section III-C.

C. Beaconing Mechanism

The proposed routing protocol uses beacons to disseminate information about a subset of the local k -hop neighborhood of a node, as detailed in Section III-B. Initially, each beacon contains only the node's information but gradually accumulates and broadcasts additional neighborhood details received from other beacons.

Each node broadcasts a new beacon at intervals defined by the beacon interval parameter. The beacon includes the sender's address a_s , position p_{a_s} , and sequence number seq_{a_s} . Each node knows its position, and the sequence number helps mitigate routing loops when a node is removed from the position table. When sending a beacon, a_s extracts $\mathcal{N}_{a_s}^1$ and $\mathcal{N}_{a_s}^2$. Using the *Random* or *FF* methods, a node selects up to m neighbors from $\mathcal{N}_{a_s}^1$. With *EFF*, a subset of $\mathcal{N}_{a_s}^1$ is chosen using d_{thr} . If fewer than m neighbors are selected from $\mathcal{N}_{a_s}^1$, the remainder is selected from $\mathcal{N}_{a_s}^2$ using the *FF* method with $\mathcal{S}_{a_s}^{\text{pre}}$ as the preselected list $\mathcal{S}_{a_s}^{\text{pre}}$. Each selected neighbor's sequence number and hop count from \mathcal{T}_{a_s} are added to the beacon.

When a beacon B_{a_s} is received, the current node a_c updates its position table \mathcal{T}_{a_c} by removing entries added via a_s that are no longer in B_{a_s} or have expired. This ensures \mathcal{T}_{a_c} is current, reflecting the latest network topology. The validity interval, t_{validity} , is set to twice the beacon interval, allowing quick response to link loss. For each neighbor a_i

in B_{a_s} , the algorithm checks if a_i is already in \mathcal{T}_{a_c} and updates a_i 's information if the beacon provides a more recent sequence number or a shorter hop count with an equal or fresher sequence. If a_i is not found, it is added as a new entry, with a_s set as the via address.

D. Forwarding Mechanism

Let a_d denote the destination node. When a node a_c sends a packet to a_d , it is assumed the position of a_d is known. For forwarding, a_c selects the neighbor a_{best} from its position table \mathcal{T}_{a_c} that offers the best advancement towards a_d . The packet is directed to $a_j = \text{via}_{a_{\text{best}}}$, a 1st order neighbor, ensuring maximal progress towards a_d . This process is illustrated in Figure 3. To mitigate issues from

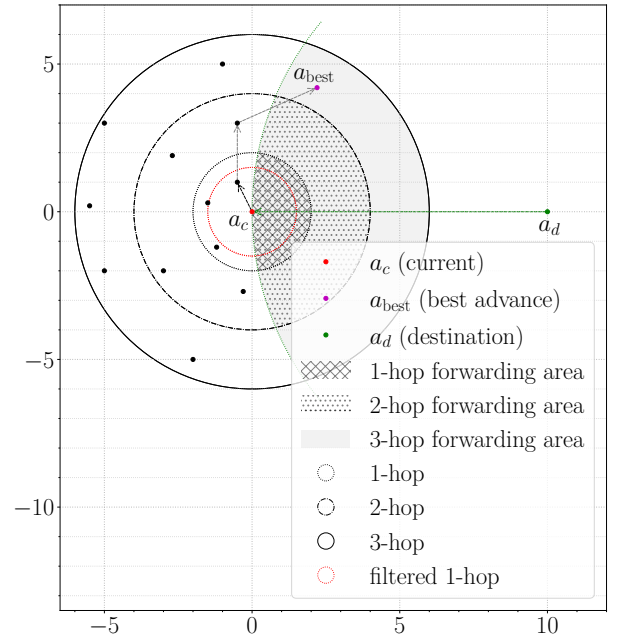


Fig. 3: The packet forwarding process, directing the packet towards $\text{via}_{a_{\text{best}}}$, the node through which a_{best} is reachable.

delayed or lost beacons, a range reduction parameter ε is introduced. This parameter restricts selection to 1st order neighbors within a radius of $r - \varepsilon$ to ensure reliability, filtering usable neighbors as illustrated in dotted red in Figure 3. The selection of ε considers nodes at the edge of the communication range moving in opposite directions as a worst-case, defined as:

$$\varepsilon = 2 \cdot \text{beacon interval} \cdot \text{average speed}. \quad (2)$$

IV. SIMULATION SETUP

This study evaluates greedy routing using subsets of the k -hop neighborhood with three selection methods: Greedy-Random, Greedy-FF, and Greedy-EFF.

A. Mobility Model

The French airspace, spanning 1 000 000 km², is modeled as a 1250 km \times 800 km rectangle (Figure 4). Aircraft can be at altitudes from 0 km to 11 km, representing various

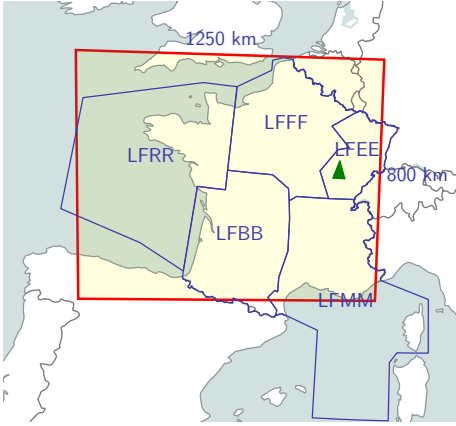


Fig. 4: The French airspace where the red outline shows the simulation boundary (generated using [10]).

flight phases. The simulation includes an average of 500 aircraft [11] and one ground station, depicted as a green triangle in Figure 4. Each aircraft selects a random position within the simulation area and moves in a straight line in a random direction. The LDACS communication range of 370.4 km is applied for A2G communication. We use an A2A communication range of 100 km, as evaluated in [11], achieving an approximate ground station connectivity ratio of 100%.

B. Network Model

1) *Data Application*: Aircraft employ Automatic Dependent Surveillance-Contract (ADS-C) technology to send their Four-dimensional (4D) positions (latitude, longitude, altitude, and time) every minute, with each packet being 34 B. This capability is essential for the safety and efficient management of future airspace [12]. The first packet of an aircraft is randomly transmitted within $[0\text{ s}, 60\text{ s}]$.

2) *Data Link Layer*: We implemented an abstract version of the MCSOTDMA, the proposed LDACS MAC layer, as specified in [4]. This implementation supports one LDACS transmitter and two receivers per aircraft, using the SH channel for beacon broadcasting and the PP channels for unicast packet transmission. The number of available PP channels adjusts dynamically based on the location, with up to 50 usable channels in this simulation [13]. Our model results in a linear increase in MAC delay on the SH channel, proportional to the number of direct neighbors, mirroring MCSOTDMA behavior [6]. As a simplification, we assume an entity with global node knowledge for optimal scheduling of transmissions. Considering MAC headers as described in [4], each beacon can accommodate up to 6 neighbor entries, each of 12 B. Hence, we evaluated subset sizes $m = 4$ and $m = 6$ for the SH channel, identifying $m = 4$ as optimal in Section II.

3) *Physical Layer*: Our simulation employs a UDG radio model, assuming a uniform communication range across all

aircraft and no channel errors. Two nodes can communicate successfully if within the defined range.

The simulation parameters are summarized in Table II.

TABLE II: Simulation Parameters

Simulation Time Limit (s)	1800
Number of Simulation Runs	50, with 95% CIs
A2G Communication Range (km)	370.4
A2A Communication Range (km)	100
Number of Aircraft	500
Aircraft Speed (km/h)	800
Simulation Area (km ²)	1 000 000
Beacon Interval (s)	5
Slot Size (s)	0.024
Packet Size (B)	34
Application Sending Rate (pkts/node/min)	1
Aircraft Density ($\times 10^{-4}$ nodes/km ²)	2.5, 3, 3.5, 4, 4.5 and 5
LDACS Equipage Fraction ρ	0.5, 0.6, 0.7, 0.8, 0.9 and 1
Subset Size m	4 and 6

V. RESULTS AND DISCUSSION

In this experiment, we vary the equipage fraction, ρ , representing the proportion of aircraft equipped with LDACS. We evaluate Greedy-Random, Greedy-FF, and Greedy-EFF algorithms at different equipage fractions, measuring their performance in terms of average Packet Delivery Ratio (PDR) and hop count. We compare their performance against Greedy-1 and Greedy-2. Although Greedy-2 includes the full neighborhood in the beacon, which exceeds the LDACS A2A slot capacity, it serves as a benchmark. The Dijkstra's algorithm is also used to demonstrate the maximum achievable PDR and minimum hop counts for each equipage fraction, despite its infeasibility here. Simulations are conducted using OMNeT++ with a communication range of 100 km and a range reduction parameter of $\varepsilon = 2.5$ km.

Greedy-Random, Greedy-FF, and Greedy-EFF improve the PDR by 1% compared to Greedy-1 at $\rho = 1$, when all aircraft are LDACS equipped as in Figure 5. At $\rho = 0.5$,

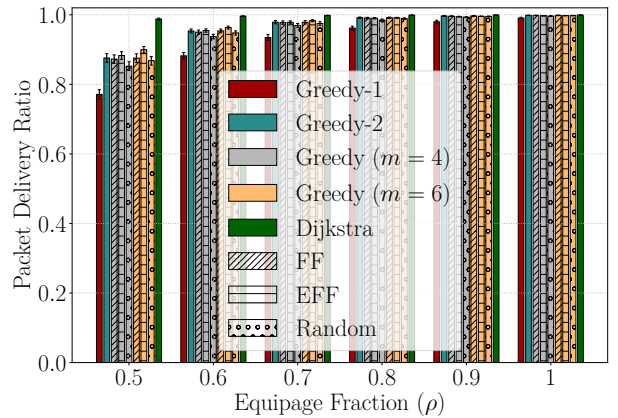


Fig. 5: Average PDR with varying equipage fraction.

these improvements increase to 11.5% for $m = 4$ and 13% for $m = 6$. Additionally, Greedy-EFF marginally

outperforms Greedy-FF on average in scenarios with lower equipage fractions due to its access to 3-hop neighborhood information. All methods with subset sizes $m = 4$ and $m = 6$ achieve performance gains comparable to Greedy-2. Despite achieving higher PDR over Greedy-1, a performance gap of at least 10% compared to Dijkstra persists at $\rho = 0.5$ due to the lack of a fallback mechanism to navigate through dead-ends, leading to packet drops.

The average hop count results over different equipage fractions are shown in Figure 6. At $\rho = 1$, Greedy-EFF,

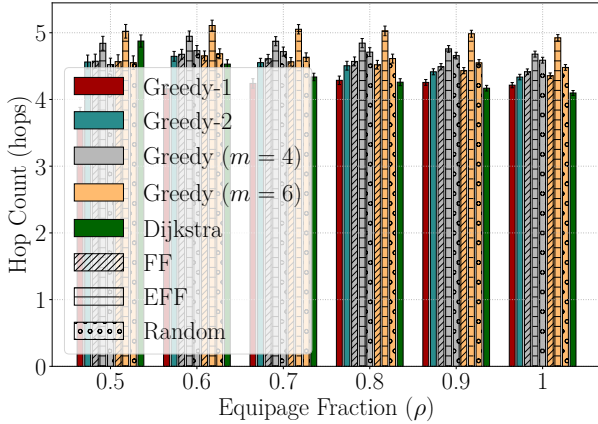


Fig. 6: Average hop count with varying equipage fraction.

which employs a 3-hop neighborhood information, exhibits slightly higher hop counts compared to its 2-hop counterparts. This increase is attributable to the broader search horizon, which may not always optimize for the maximum advancement per hop, potentially leading to longer routes. As ρ decreases, the difference in hop counts diminishes. Overall, the hop counts for all methods, including Greedy-EFF, are comparable to those of Greedy-2 and are on average up to 0.82 hops higher than those achieved by Dijkstra at $\rho = 1$.

Following the previous analysis, we now evaluate the *Random*, *FF*, and *EFF* algorithms in terms of selecting k^{th} order neighbors. We define the Capture Ratio as the ratio of unique k^{th} order neighbors identified by each method against the actual total, averaging this across all nodes. Our simulations involve 50 random mobility snapshots conducted in an area large enough to mitigate edge effects, reflecting the density and equipage fractions from the previous scenario. Using a subset size of $m = 4$ achieves a balance of coverage gain over overlap, as shown in Figure 5. We present how this subset size influences the average capture ratio of 2nd and 3rd order neighbors. The results in Figure 7 indicate that at a node density of 5×10^{-4} nodes/km² and with $m = 4$, the *FF* method achieves a capture ratio of 0.6 for 2nd order neighbors, compared to 0.52 by *Random*, marking a 15.4% improvement. *Random* selection becomes less effective at higher densities due to an enlarged selection pool. At 2.5×10^{-4} nodes/km², the *FF* method achieves a capture ratio of 0.7, compared to 0.64 by *Random*, reflecting a 9.3% improvement. With an average of 7.6 first-order

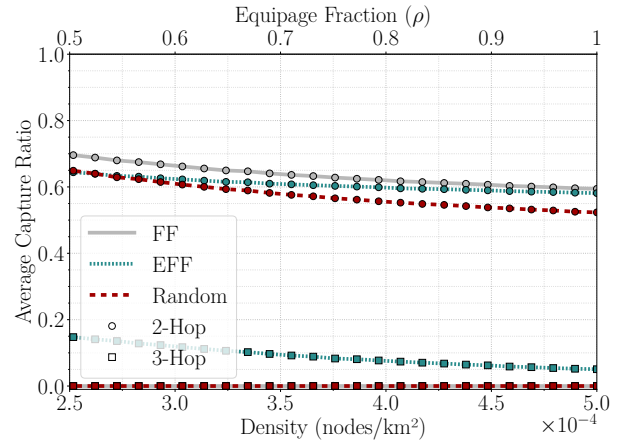


Fig. 7: Average k^{th} order neighbors capture ratio for 100 km communication range with subset size $m = 4$.

neighbors, selecting just four means *Random*'s performance remains effective. Additionally, at this density, *EFF* achieves the same performance as *Random* by strategically sacrificing some 2nd order neighbors to capture 15% of 3rd order neighbors, a capability not present in *FF* or *Random*. At a higher density of 5×10^{-4} nodes/km², despite selecting fewer 1st order neighbors than *Random*, *EFF* achieves a 2nd order neighbor capture ratio of 0.582, compared to 0.52 by *Random*, marking a 12% improvement, and it also captures 5.1% of 3rd order neighbors. As density increases, *EFF*'s performance is expected to align more closely with *FF* due to the minimal effect of the distance threshold.

With $m = 6$, the average 2nd order neighbors capture ratios for *FF*, *EFF*, and *Random* range between $[0.84, 0.7]$, $[0.70, 0.61]$, and $[0.83, 0.67]$ respectively (Figure 8). Additionally, *EFF* captured 34.6% of 3rd order neighbors at 2.5×10^{-4} nodes/km² and 25.8% at 5×10^{-4} nodes/km².

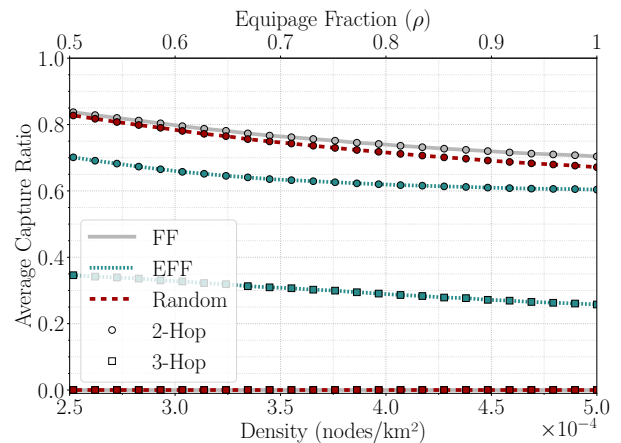


Fig. 8: Average k^{th} order neighbors capture ratio for 100 km communication range with subset size $m = 6$.

VI. RELATED WORK

Sparse networks exacerbate dead-end situations, leading to the exploration of greedy forwarding strategies that include 2-hop or 3-hop neighborhood information [9], [14]. However, The performance gain from Greedy-2 is higher than from Greedy-3 [14]. While this approach mitigates routing inefficiencies, it significantly increases beacon size, an issue not fully addressed in previous studies. The slot-based MAC protocol in LDACS A2A communications complicates beacon size management within strict slot durations. Studies like [8], [15] show that including direct neighbors in the beacon doubles the overhead ratio compared to Greedy-1, without considering the necessary beacon size reduction for slot duration compliance.

Addressing the beacon size challenge, existing literature aimed to reduce message counts for capturing 2-hop neighborhood information using $O(n)$ messages of $O(\log n)$ bits each, where n is the number of nodes in the network [16]. However, this approach focuses on message efficiency rather than direct beacon size reduction. Further advancements used probabilistic structures like Bloom filters to compress the neighbor list [17]–[19]. These methods efficiently encapsulate all direct neighbors and can accommodate k -hop neighborhoods, enhancing broadcasting protocols but lacking the positional information required for geographic Greedy- k routing.

Our investigation proposes a solution addressing both the need for a fixed maximum beacon size including a subset of direct neighbors with positional information and the constraints of LDACS A2A MAC, which accommodates approximately an additional 72 B in the beacon after headers. This constraint influences the feasible number of neighbors in a beacon, based on entry size, e.g., 12 B in our case as specified in Section III-A. Our method aims to select nodes within this subset to optimally enhance performance, achieving Greedy-2 forwarding gains within LDACS A2A communication slot durations. To the best of our knowledge, our approach is the first to reduce beacon size by selecting a subset of the neighborhood and including both MAC addresses and positional information in the beacon, offering a novel contribution to the field.

VII. CONCLUSION

We presented a novel approach to enhance greedy forwarding in sparse networks by leveraging 3-hop neighborhood information. We proposed three methods for selecting subsets of k^{th} order neighbors: *Random*, *FF*, and *EFF*, and derived an optimal fixed subset size for performance improvements with Greedy-2 forwarding. We found that a subset size of 4 is optimal, balancing coverage and overlap.

Our simulation study evaluated the proposed routing protocol and selection methods over the French airspace with varying equipage fractions. We assessed average PDR, hop count, and capture ratio of k^{th} order neighbors. Our methods outperform Greedy-1, especially in improving PDR in sparse scenarios prone to dead-ends. All proposed methods enhance

PDR by up to 13% relative to Greedy-1, achieving Greedy-2 performance gain. Additionally, Greedy-FF captures more 2nd order neighbors on average than Greedy-Random and Greedy-EFF, while Greedy-EFF can capture up to 34.6% of 3rd order neighbors. All models were implemented using OMNeT++ and Python, with details available as open-source for the research community in [20].

This approach offers potential benefits for geographical routing beyond aeronautical communication, especially in low-density large networks where greedy forwarding often hits dead-ends. Enhanced neighborhood awareness can be applied in load balancing by capturing the load status of 2nd and 3rd order neighbors. Furthermore, our method's partial k -hop neighborhood awareness lays the groundwork for developing effective strategies when a k -hop neighborhood is insufficient, and can be adapted for k -hop neighborhoods and 3D networks by adjusting the subset size m .

REFERENCES

- [1] Eurocontrol, "Aviation Outlook 2050," Main Report, Apr. 2022. (visited on 10/28/2023).
- [2] "White paper: Ubiquitous aviation connectivity with LDACS," FRE-QUENTIS AG, Technical Report, 2021. (visited on 10/28/2023).
- [3] M. A. Bellido-Manganell and M. Schnell, "Towards Modern Air-to-Air Communications: The LDACS A2A Mode," in *2019 IEEE/AIAA 38th Digital Avionics Systems Conference (DASC)*, Sep. 2019, pp. 1–10. DOI: 10.1109/DASC43569.2019.9081678. (visited on 10/28/2023).
- [4] S. Lindner, K. Fuger, M. A. E. Ahmed, A. Timm-Giel, J. Hampel, and M. Bellido, "MCSOTDMA Protocol Specification," Zenodo, Tech. Rep., Jun. 2023. DOI: 10.5281/zenodo.8079189. (visited on 03/31/2024).
- [5] D. Medina, F. Hoffmann, F. Rossetto, and C.-H. Rokitsansky, "A Geographic Routing Strategy for North Atlantic In-Flight Internet Access Via Airborne Mesh Networking," *IEEE/ACM Transactions on Networking*, vol. 20, no. 4, pp. 1231–1244, Aug. 2012. DOI: 10.1109/TNET.2011.2175487.
- [6] S. Lindner, K. Fuger, M. A. E. Ahmed, and A. Timm-Giel, "Multi-Channel Self-Organized TDMA for Future Aeronautical Mobile Ad-Hoc Networks," *IEEE Transactions on Vehicular Technology*, pp. 1–15, 2024. DOI: 10.1109/TVT.2024.3380316. (visited on 03/31/2024).
- [7] D. Medina, F. Hoffmann, F. Rossetto, and C.-H. Rokitsansky, "A Geographic Routing Strategy for North Atlantic In-Flight Internet Access Via Airborne Mesh Networking," *IEEE/ACM Transactions on Networking*, vol. 20, no. 4, pp. 1231–1244, Aug. 2012. DOI: 10.1109/TNET.2011.2175487. (visited on 04/03/2024).
- [8] M. Y. Arafat and S. Moh, "A Q-Learning-Based Topology-Aware Routing Protocol for Flying Ad Hoc Networks," *IEEE Internet of Things Journal*, vol. 9, no. 3, pp. 1985–2000, Feb. 2022. DOI: 10.1109/JIOT.2021.3089759. (visited on 10/15/2023).
- [9] J. Zhou, Y. Chen, B. Leong, and P. Sundaramoorthy, "Practical 3D geographic routing for wireless sensor networks," in *SenSys 2010 - Proceedings of the 8th ACM Conference on Embedded Networked Sensor Systems*, 2010, pp. 337–350. DOI: 10.1145/1869983.1870016.
- [10] X. Olive, "Traffic, a toolbox for processing and analysing air traffic data," *Journal of Open Source Software*, vol. 4, no. 39, p. 1518, Jul. 2019. DOI: 10.21105/joss.01518. (visited on 04/16/2024).
- [11] Q. Vey, A. Pirovano, J. Radzik, and F. Garcia, "Aeronautical Ad Hoc Network for Civil Aviation," in *Communication Technologies for Vehicles*, A. Sikora, M. Berbineau, A. Vinel, M. Jonsson, A. Pirovano, and M. Aguado, Eds., Cham: Springer International Publishing, 2014, pp. 81–93. DOI: 10.1007/978-3-319-06644-8_8.
- [12] J. Valle Martinez, "Network 4D Trajectory CONOPS," Technical Report 23/08/28/46, Sep. 2023. (visited on 03/29/2024).

- [13] M. A. Bellido-Manganell and M. Schnell, "Feasibility of the Frequency Planning for LDACS Air-to-Air Communications in the L-Band," in *2021 Integrated Communications Navigation and Surveillance Conference (ICNS)*, Apr. 2021, pp. 1–14. DOI: 10.1109/ICNS52807.2021.9441623. (visited on 03/31/2024).
- [14] C. S. Chen, Y. Li, and Y.-Q. Song, "An exploration of geographic routing with k-hop based searching in wireless sensor networks," in *2008 Third International Conference on Communications and Networking in China*, Aug. 2008, pp. 376–381. DOI: 10.1109/CHINACOM.2008.4685045. (visited on 11/26/2023).
- [15] Y. Li, C. S. Chen, Y.-Q. Song, Z. Wang, and Y. Sun, "Enhancing Real-Time Delivery in Wireless Sensor Networks With Two-Hop Information," *IEEE Transactions on Industrial Informatics*, vol. 5, no. 2, pp. 113–122, May 2009. DOI: 10.1109/TII.2009.2017938. (visited on 11/26/2023).
- [16] G. Calinescu, "Computing 2-Hop Neighborhoods in Ad Hoc Wireless Networks," in *Ad-Hoc, Mobile, and Wireless Networks*, S. Pierre, M. Barbeau, and E. Kranakis, Eds., ser. Lecture Notes in Computer Science, Montreal, Canada: Springer, 2003, pp. 175–186. DOI: 10.1007/978-3-540-39611-6_16.
- [17] K. C. Lee, U. Lee, and M. Gerla, "Geo-opportunistic routing for vehicular networks," *IEEE Communications Magazine*, vol. 48, no. 5, pp. 164–170, May 2010. DOI: 10.1109/MCOM.2010.5458378. (visited on 01/31/2024).
- [18] K. Na Nakorn, Y. Ji, and K. Rojviboonchai, "Bloom Filter for Fixed-Size Beacon in VANET," in *2014 IEEE 79th Vehicular Technology Conference (VTC Spring)*, Seoul, South Korea: IEEE, May 2014, pp. 1–5. DOI: 10.1109/VTCSpring.2014.7022849. (visited on 01/31/2024).
- [19] F. Klingler, R. Cohen, C. Sommer, and F. Dressler, "Bloom Hopping: Bloom Filter Based 2-Hop Neighbor Management in VANETs," *IEEE Transactions on Mobile Computing*, vol. 18, no. 3, pp. 534–545, Mar. 2019. DOI: 10.1109/TMC.2018.2840123. (visited on 11/26/2023).
- [20] M. Ahmed and K. Fuger, *LDACS Greedy K-Hop Simulator*, Zenodo, Jul. 2024. DOI: 10.5281/zenodo.12911062. (visited on 04/19/2024).